Carbohydrate Polymers 88 (2012) 465–473

Contents lists available at SciVerse ScienceDirect

Carbohydrate Polymers

journal homepage: www.elsevier.com/locate/carbpol

Synthesis and characterization of thermo- and pH-responsive bacterial cellulose/acrylic acid hydrogels for drug delivery

Mohd Cairul Iqbal Mohd Amin[a,*], Naveed Ahmad[a], Nadia Halib[b], Ishak Ahmad[c]

[a] Faculty of Pharmacy, Universiti Kebangsaan Malaysia, Jalan Raja Muda Abdul Aziz, 50300 Kuala Lumpur, Malaysia
[b] Medical Technology Division, Malaysian Nuclear Agency, Bangi, 43000 Kajang, Selangor, Malaysia
[c] Faculty of Science and Technology, Universiti Kebangsaan Malaysia, 43600 UKM, Bangi, Selangor, Malaysia

ARTICLE INFO

Article history:
Received 20 August 2011
Received in revised form 8 December 2011
Accepted 13 December 2011
Available online 30 December 2011

Keywords:
Acrylic acid
Bacterial cellulose
Drug-delivery system
Electron-beam irradiation
Hydrogel
Swelling behavior

ABSTRACT

To assist in identifying the utility of novel materials in drug-delivery applications, this study investigated the use of bacterial cellulose (BC), a natural biopolymer, in the synthesis of hydrogels for drug-delivery systems. BC was combined with different proportions of acrylic acid (AA) to fabricate hydrogels by exposure to accelerated electron-beam irradiation at different doses. Fourier transform infrared analysis revealed that the AA had been successfully grafted onto the cellulose fibers and allowed for prediction of the reaction mechanism in the synthesis of hydrogels. Thermal and morphological characterization indicated the formation of thermally stable hydrogels with pore size determined by AA content and irradiation dose. The results of swelling and in vitro drug-release studies revealed the hydrogels to be both thermo- and pH-responsive. Such thermo- and pH-responsiveness, in addition to their morphological characteristics, suggests that these BC/AA hydrogels are promising candidates as controlled drug-delivery systems.

1. Introduction

The conventionally passive role of pharmaceutical excipients in pharmaceutical products as providers of weight, volume, flowability, and consistency is rapidly evolving to the more active roles of drug-performance enhancers that target drug delivery at the site of action and protect the drug from degradation inside the body (Beneke, Viljoen, & Hamman, 2009; Guenther, Smirnova, & Neubert, 2008). This evolution has prompted researchers to discover and explore new materials for drug-delivery applications. From the application point of view, many natural polymers, such as starch, cellulose, chitosan, carrageenan, and alginate, have been explored due their stability, availability, sustainability and low level of toxicity (Malafaya, Silva, & Reis, 2007; Säkkinen, Seppälä, Heinänen, & Marvola, 2002). These biopolymers also offer the advantages of biodegradability, biocompatibility, and capability of chemical modification which confers them principle properties for their application to drug-delivery systems (Domb & Kost, 1997). While many successful drug-delivery systems have been developed using conventional biopolymers, the rapid evolution of the pharmaceutical industry demands continued exploration to identify novel biomaterials that can be used in devising intelligent drug-delivery systems with efficient in vivo performance.

One such biopolymer of great interest is bacterial cellulose (BC) synthesized by *Acetobacter xylinum*. BC possesses many unique structural and biochemical properties, including an ultrafine nanofibrous network structure (Patel & Suresh, 2008), bioadaptibility (Hong & Qiu, 2008), chemical stability, and non-toxicity (Grzegorczyn & Slezak, 2007; Moreira et al., 2009). Due to its uniform and ultrafine fibrous network structure, BC has excellent water-absorbance capacity and mechanical properties, including high tensile strength and elastic modulus (Czaja, Young, Kawecki, & Brown, 2008; Hua et al., 2009; Tatsuya, Sachiko, Kaoru, & Yoshinari, 2011). These advantageous properties make BC an attractive material for the fabrication of intelligent adsorptive materials for drug-delivery applications, such as hydrogels.

Hydrogels are adsorptive materials composed of hydrophilic polymers linked through chemical or physical crosslinking in such a manner that they can absorb and retain large volumes of water within their three-dimensional network without dissolution. In addition to being thermo responsive, they can be fabricated to become pH responsive by the addition of acrylic acid (AA). Such pH- and thermo-responsiveness, in addition to their swelling capacity and biocompatibility, allows hydrogels to serve as versatile materials in many biomedical and pharmaceutical applications. Such applications include the delivery of antibodies, antibiotics, enzymes, hormones, and contraceptives that act through a variety of routes, including oral, subcutaneous, and intramuscular routes. These characteristics allow hydrogels to play important roles in sustained-release, controlled-release, targeted-release, and

* Corresponding author. Tel.: +60 3 9289 7690; fax: +60 3 2698 3271.
E-mail address: mciamin@pharmacy.ukm.my (M.C.I. Mohd Amin).

0144-8617/$ – see front matter.
doi:10.1016/j.carbpol.2011.12.022

protective drug-delivery systems (Hamidi, Azadi, & Rafiei, 2008; Hennink, De Jong, Bos, Veldhuis, & Van Nostrum, 2004; Peppas, Bures, Leobandung, & Ichikawa, 2000). Nevertheless, their great potential has been hampered by one major challenge: the difficulty of fabricating sufficiently mechanically strong hydrogels using conventional chemical crosslinking methods without compromising their intelligent-swelling characteristics (Haraguchi, Takehisa, & Fan, 2002; Karaaslana, Tshabalalab, Yelleb, & Buschle-Diller, 2011).

Electron-beam radiation (ionizing radiation) can initiate crosslinking that produces pure, sterile, and residue-free hydrogels. Unlike conventional chemical crosslinking methods, this method does not require the addition of catalysts or any other additives to modify the material in a manner that protects the inherent biocompatible and biodegradable properties of natural polymers (Hennink & van Nostrum, 2002). Moreover, electron-beam radiation requires no involvement of a radioactive source, eliminating the risk of hazardous toxicity due to the formation of radioactive substances. Using this method, the degree of crosslinking and the pore size of hydrogels, which strongly determine the extent of swelling, can be easily controlled by varying the irradiation dose (Anjali, Manohar, Sabharwalb, Bhardwajb, & Majalib, 2000; Said, Abd Alla, El-Naggar, 2004). As such, this method has been found to be very useful in preparing hydrogels for pharmaceutical applications in which even a low level of contamination is undesirable.

The aim of this work was to investigate the use of novel materials in drug-delivery applications by synthesis and characterization of thermo- and pH-responsive hydrogels for use in controlled drug-delivery systems. BC was combined with AA at several ratios to fabricate hydrogels by exposure to accelerated electron-beam irradiation at different doses. After fabrication, FT-IR, thermal and morphological characterization of the hydrogels was performed to investigate the structure, stability and the porosity of the hydrogels. This characterization was followed by both swelling and in vitro drug-release studies to evaluate the thermal and pH responsiveness of the hydrogels and their overall potential as drug-delivery systems.

2. Experimental

2.1. Materials

Bacterial cellulose (BC) was prepared from *nata de coco* that had been purified, lyophilized, ground, characterized, and then identified as described in British Pharmacopeia (2010). Acrylic acid (AA), bovine serum albumin (BSA), and phosphate buffer saline (PBS) were supplied by Sigma–Aldrich, USA. Simulated gastric fluid (SGF) and simulated intestinal fluid (SIF) without enzymes were prepared according to the procedure described by the United States Pharmacopeia (2010). Distilled water was used to prepare aqueous solutions and dispersions, and 12 cm × 12 cm × 0.5 cm plastic trays were used as molds for the preparation of the hydrogels.

2.2. Synthesis of BC/AA hydrogels

Lyophilized BC was ground to a powder of particle size ranging from 20 to 200 μm. AA was added to a 1% (w/v) dispersion of BC in distilled water to make 20:80, 30:70, and 40:60 AA:BC mixtures. To ensure thorough mixing, each mixture was stirred by a mechanical homogenizer (IKA Labortechink Ultra Turrax T25, Germany) for 30 min, then poured into a mold for subjection to electron-beam radiation of 35 or 50 kGy in air at the accelerator facility (EPS-3000, Japan) of the Malaysian Nuclear Agency. The resulting hydrogels were named as 208035, 208050, 307035, 307050, 406035, and 406050 hydrogels, on the basis of AA:BC ratio and electron-beam irradiation dose.

2.3. Gel fractions of hydrogels

Freshly prepared hydrogels were cut into disks 1 cm in diameter and 2 mm in thickness and dried in an oven at 60 °C to a constant weight. The dried hydrogels were then subjected to extraction in distilled water at ambient temperature for 7 days to remove free BC and AA, after which the extracted hydrogels were dried in an oven at 60 °C to a constant weight. The percent gel fraction was calculated using the following equation:

$$\frac{G_d}{G_i} \times 100 \quad (1)$$

where G_d is the initial dried weight before extraction and G_i is the constant dried weight of the hydrogels after extraction.

2.4. FT-IR analysis

FT-IR analysis was conducted to identify the structure of the hydrogels using the Perkin Elmer FT-IR Spectra 2000. Hydrogels were cut into 1 cm × 1 cm × 2 mm thin films, directly placed on the top plate of a diamond attenuated total reflection (ATR) and scanned over a range of 4000–500 cm^{-1}.

2.5. Thermogravimetric analysis

A Perkin Elmer STA 6000 was used to perform thermogravimetric analysis (TGA) of the BC, AA, and hydrogels. In preparation for TGA, the hydrogels were ground to powder form. Approximately 10 mg of BC, AA, and hydrogel powder was placed in the sample pan for analysis over a temperature range of 50–900 °C at a heating rate of 10 °C/min under a nitrogen purge (25 mL/min). The differential thermogravimetric (DTG) curve was derived from the TGA results using the Pyris 1 software program.

2.6. Differential scanning calorimetry

The glass-transition temperatures (T_g) of the purified hydrogels were determined using a Perkin Elmer Diamond differential scanning calorimeter to perform differential scanning calorimetry (DSC). Approximately 10 mg of all samples was sealed in a standard aluminum pan. The analysis was conducted over a temperature range of 0–150 °C at a 20 °C/min heating rate under a nitrogen purge (20 mL/min).

2.7. Morphological analysis

The morphologies of the porous structure of the BC/AA hydrogels were examined by scanning-electron microscopy (SEM). To prepare the hydrogel samples for examination under a Leo1450 VP (Germany) SEM, they were mounted on an aluminum stub with double-sided carbon tape and coated with gold in sputter coater (SC500; BioRad, UK) under argon atmosphere.

2.8. Swelling studies

To measure the swelling ratio (SR), dried and weighed hydrogels disks were immersed into 50 mL solutions of PBS at different pH values (2–10) and temperatures (25–50 °C). The swollen samples were weighed during time intervals at which excess of buffer was removed by blotting with filter paper. The SR percent was calculated using the following equation:

$$SR\% = \frac{G_s - G_d}{G_d} \times 100 \quad (2)$$

where G_s and G_d are the weights of swollen and dried hydrogels, respectively. The experiments were performed in triplicate and the average of results was reported.

2.9. Drug loading

Bovine serum albumin (BSA) was loaded as a model drug into the 208050, 208035 and 307050 hydrogels using the swelling-diffusion method. The BSA solutions (0.5 and 1%, w/v) were prepared in PBS at pH 7.4. Dried and weighed hydrogel disks were then immersed in 25 mL of the BSA solutions and incubated at 37 °C. After 2 days, the hydrogels were removed from the solution, washed with SGF (pH 1.2), and dried under vacuum at 25 °C to a constant weight. The remaining solution was diluted to 50 mL and the amount of BSA left in the loading solution was determined by spectrophotometry (UV-1601; Shimadzu, Japan) at a wavelength of 280 nm. BSA entrapment efficiency (EE) in the hydrogels was calculated by using the following equation:

$$\mathrm{EE} = \frac{W_o - W_f}{W_o} \times 100 \quad (3)$$

where W_o is the total amount of BSA in solution before loading and W_f is the total amount of BSA in solution after loading.

2.10. In vitro drug release studies

In vitro drug release profiles of the hydrogels were obtained by immersing BSA-loaded hydrogel samples into 25 mL of SGF (pH 1.2) for 2 h and then in SIF until maximum release. The samples were incubated at 37 °C with constant agitation (50 rpm). After a predetermined period, 0.5 mL samples were removed from the release medium and replaced with fresh medium. The concentration of BSA in samples was measured using a UV/vis spectrophotometer at 280 nm, according to the standard BSA calibration curve. All release studies were performed in triplicate and the means of all measurements calculated. The results were presented in terms of cumulative percentage release as a function of time using the following formula:

$$\text{Cumulative percentage release} = \frac{W_t}{W_l} \times 100 \quad (4)$$

where W_t is the amount of BSA released from the hydrogel at time t and W_l is the amount of BSA loaded onto the hydrogel.

3. Results and discussion

3.1. Hydrogel synthesis

The minimum gelation dose for polyacrylic acid (PAA) alone has been reported as 50 kGy (El-Naggar, Abd Alla, & Said, 2006). However, the results of the present study suggested that 35 kGy is the lowest dose required to solidify the hydrogels of 0.5 cm thickness without any elevation of temperature that could produce bubbles in the hydrogel matrices. The production of bubbles is to be avoided because it could influence the mechanical properties of a hydrogel, which may interrupt drug release when the hydrogel is used as a drug-delivery carrier.

3.2. Gel fractions

The gel fractions of the hydrogels are shown in Table 1. As can be observed, the fractions increased in tandem with the addition of an increasing amount of AA into the gel formulation, which resulted in increased polymerization of AA into polyacrylic acid (PAA) by electron-beam radiation. The extracted weight and gel fractions were also influenced by the irradiation dose. Among hydrogels of the same initial formulation, those exposed to a higher dose of electron-beam irradiation yielded a higher extracted weight and gel fraction, suggesting that a higher dose results in a more highly crosslinked and insoluble network. Moreover, electron-beam irradiation, which led to the radiolysis of water, resulted in the production of electrons, hydroxyl radicals, hydrogen atoms, and reactive species, which likely led several reactive sites on the AA to become crosslinked. This likely scenario suggests that a greater number of reactive species are produced with higher doses of irradiation, which increases the degree of crosslinking (Said et al., 2004), and allows for the conclusion that the gel fraction of hydrogels is influenced by both the irradiation dose and the quantity of AA.

Table 1
Gel fractions of BC/AA hydrogels.

Samples	Initial weight (G_i)	Extracted weight (G_o)	% gel fraction
208035	12.16 ± 1.180	7.81 ± 0.839	60.21 ± 3.440
208050	12.48 ± 0.974	9.64 ± 0.777	77.23 ± 1.170
307035	19.78 ± 1.477	17.15 ± 1.206	86.75 ± 0.510
307050	20.75 ± 0.510	19.02 ± 0.486	91.69 ± 1.544
406035	27.08 ± 0.141	24.61 ± 0.178	90.86 ± 0.206
406050	27.36 ± 0.445	25.92 ± 0.437	94.74 ± 0.164

3.3. FT-IR analysis

As FT-IR spectroscopy is an effective tool for studying the molecular structure of polymers, the FT-IR spectra of the BC, AA, and hydrogel composites were obtained. As can be observed in Fig. 1, although the hydrogels shared the same peaks, the peaks were of varying intensities, suggesting that similar interactions

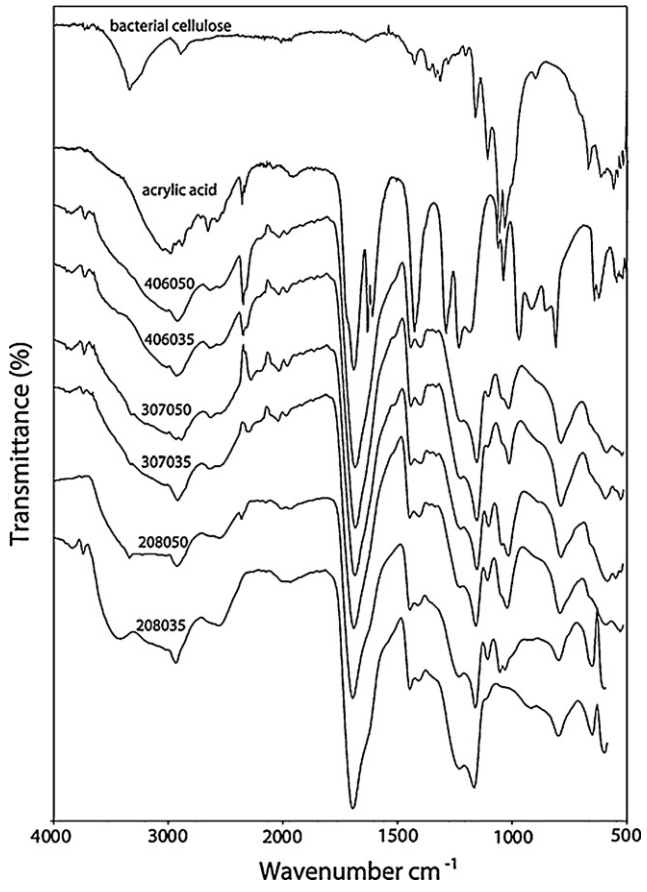

Fig. 1. FT-IR spectra of BC, AA, and BC/AA hydrogels.

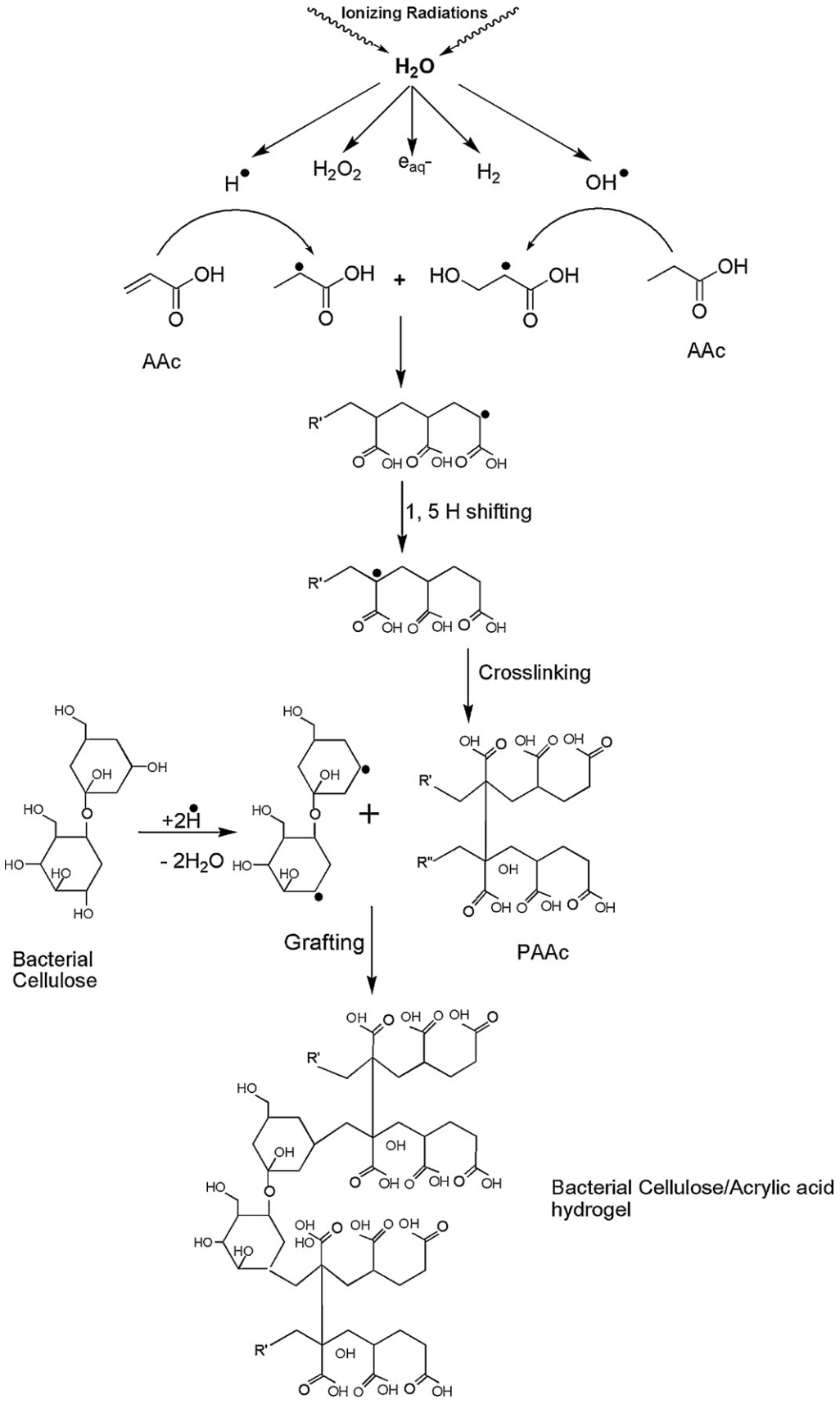

Fig. 2. Reaction mechanism involved in hydrogel synthesis.

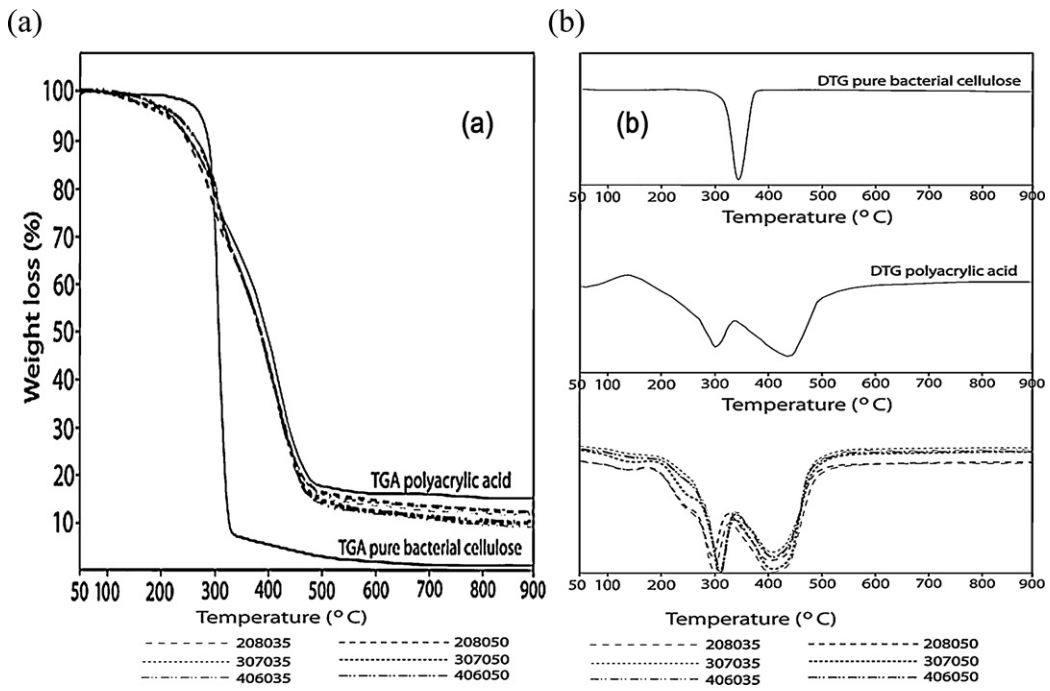

Fig. 3. TGA (a) and DTG (b) of BC, PAA, and hydrogels.

occurred between the BC fibers and the AA during the formation of the hydrogels. The BC FT-IR spectra exhibited a C—O stretching vibration at 1040 cm^{-1}, a C—O—C stretch of the ether linkage (1,4-β-D-glucoside) of cellulose at 1163 cm^{-1}, a C—H stretch at 2926 cm^{-1}, and an O—H stretch of intermolecular hydrogen bonding at 3440 cm^{-1}. The AA spectra exhibited distinctive peaks at 1600 cm^{-1} due to C=C stretching and at 1700 cm^{-1} due to C=O stretching, as well as a broad peak at 3040–2340 cm^{-1} due to O—H stretching (Pavia, Lampman, & Kriz, 2001). Such C=C stretching as a shoulder in the hydrogel spectra indicates the polymerization of AA into PAA, an indication supported by the finding that irradiation of acrylates with electrons leads to the curing of the polymer by the formation of radicals that initiate polymerization and crosslinking reactions (Scherzer, Beckert, Langguth, Rummel, & Mehnert, 1998; Takács, Dajka, & Wojnárovits, 2001). Moreover, the absence of C—O stretching vibrations in the hydrogel spectra indicated the grafting of AA onto BC fibers.

3.4. Reaction mechanism

The reaction mechanism involved in the hydrogel synthesis is illustrated in Fig. 2. During the irradiation process, the water molecules were converted into reactive species, such as electrons, hydroxyl radicals, and hydrogen atoms (Strauss, Knolle, & Naumov, 1998), that created active sites on the AA and BC for grafting. The presence of a C=O stretching vibration at approximately 1700 cm^{-1} in the hydrogel FT-IR spectra was clearly due to the presence of a carboxylic group from AA, while a very broad peak at approximately 3500–2500 cm^{-1} indicates the presence of extensive hydrogen bonding. This vibration reflects the increased hydrogen bonding of BC with the AA polymerization, with bonds being formed between the carboxylic group of AA and the non-substituted hydroxyl group of the BC (Said et al., 2004).

In accordance with the expectation that all reactive transients from water react with AA monomers during the radiolysis of water, water radiolysis in this study resulted in the formation of radicals that initiated the polymerization of AA into PAA (Strauss et al., 1998). The formation of the mid-chain radicals (crosslinked sites) by the intermolecular 1,5 H-shift, which has been observed in electron-pulse radiolysis (EPR) investigations of acrylates (Ulański, Bothe, Rosiak, & von Sonntag, 1994), could be the pathway by which PAA crosslinks with BC during the irradiation process. The OH and H radicals are also known to be capable of extracting hydrogen atoms from polymers when addition to the double bond is not possible (Said et al., 2004).

3.5. Thermogravimetric analysis

Thermogravimetric analysis (TGA) was conducted to examine the effect of composition and irradiation dose on the thermal decomposition of the BC/AA hydrogels. As evident from the TG and DTG curves of BC, PAA, and hydrogels shown in Fig. 3, BC underwent single-step decomposition, with maximum decomposition occurring at 343 °C. These results are in agreement with previous reports and confirm the purity of the cellulose extracted from *nata de coco* (Huang & Li, 1998; Nada & Hassan, 2007). In contrast, the TG and DTG curves show that the PAA underwent a stepwise decomposition, with peaks occurring at 301 °C and 425 °C. In the three-step decomposition of PAA, the first step is predominantly associated with the release of H_2O; the second with a loss in mass from the release of H_2O, CH_4, and the AA monomer at approximately 330 °C; and the third with a loss in mass between 350 °C and 500 °C due to the release of AA moieties consisting of short-chain fragments from depolymerization (Dubinsky, Grader, Shter, & Silverstein, 2004).

The thermal decomposition data of the hydrogels shown in Fig. 3 demonstrate that the hydrogels underwent three stages of decomposition similar to those of the PAA. The sharp and deep decomposition peaks at 300 °C resemble the BC decomposition peak, suggesting that initiation of BC decomposition in the hydrogel composites began at a lower temperature, falling from 343 °C to 300 °C, due to grafting of PAA (Huang & Li, 1998). Likewise, the decomposition peak of AA moieties occurred between 406 °C and 410 °C instead of at 425 °C. This decrease was the result of a part of the AA monomer being grafted onto the BC to produce branched structure. The resultant combination of branched and linear structures made the hydrogels less crystalline and thermally

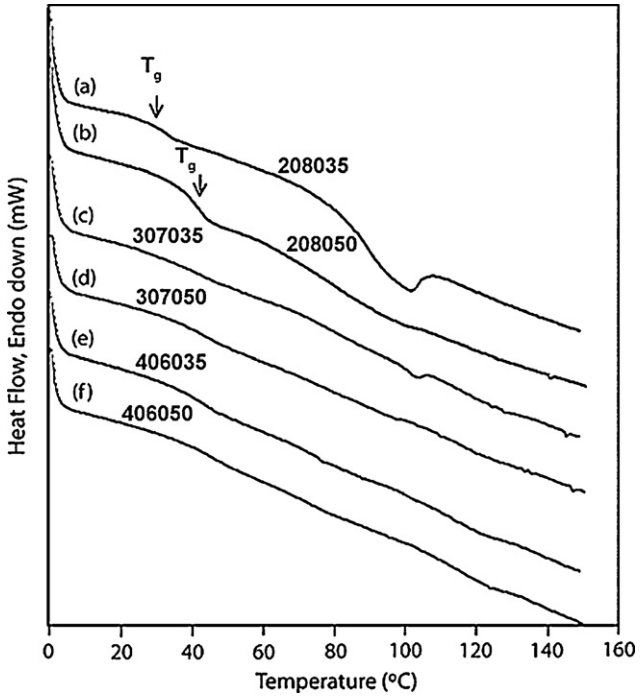

Fig. 4. DSC curves of hydrogels; arrows indicate T_g positions.

stable, facilitating their degradation at lower temperatures. This branched structure also facilitated chain scission of PAA, enabling decomposition of AA moieties at lower temperatures. The finding that the 406050 hydrogel exhibited a higher decomposition temperature than the 208035 hydrogel demonstrates that the addition of a greater quantity of AA produces a greater number of highly crosslinked and compact structures, which have a higher degree of thermal stability.

3.6. Differential scanning calorimetry

Differential scanning calorimetry (DSC) curves of the BC/AA hydrogels are shown in Fig. 4. The glass transition temperatures (T_g) of the 208035 and 208050 hydrogels were found to be 39 °C and 41 °C, respectively, with an endothermic peak observed between 80 and 100 °C for the 208035 hydrogel. As H_2O molecules bind to cellulose, acting as a plasticizer and influencing the reduction in T_g, the higher cellulose content of the 208035 hydrogel resulted in its T_g being much lower than that of both BC (220–250 °C) (Wang, Luo, Peng, & Pei, 2008) and PAA (106 °C) (Chan & Chu, 2001). Although the 208050 hydrogel contained the same amount of BC as the 208035 hydrogel, it was crosslinked at higher irradiation dose (50 kGy), which polymerized the PAA to longer chains and grafted more PAA onto the BC fibers to form a more condensed and rigid structure. Such increased interaction between the polymer chains decreased the ability of the moisture to bind with the hydrogels (Szczesniak, Rachocki, & Tritt, 2008). As a result, a very low amplitude of the endothermic peak was observed for the 208050 hydrogel. The polymerization of PAA into longer chains and the grafting of PAA to BC also increased the molecular weight of the material. As large molecules require more energy and higher temperatures to move, they exhibit higher T_g values (Gabbott, 2008).

The additional finding that the DSC curves for the 208035 and 208050 hydrogels exhibited only one T_g peak suggests that BC/AA hydrogels proceed through a miscible homogenous amorphous phase (Lau & Mi, 2002). As it contained slightly less BC than the 208035 hydrogel, the 307035 hydrogel exhibited a small endothermic peak between 100 °C and 105 °C. In contrast, the 307050 hydrogel exhibited no endothermic peak, as the intensive interactions between the polymer chains may have prevented moisture from binding in the polymer matrix. Similarly, no endothermic peak was observed for the 406035 and 406050 hydrogels due to their low BC content and high crosslinking density in the presence of a greater quantity of PAA. Changes in the slope of the DSC baselines for the 307035, 307050, 406035, and 406050 hydrogels were so broad that their T_g values were difficult to determine. These broad baselines suggest that the hydrogels consist of a combination of an amorphous and partially crystalline materials which are together referred to as a rigid amorphous fraction (Gabbott, 2008). In this fraction, the amorphous component is not completely free to move due to its close proximity to the crystalline materials, preventing it from undergoing the glass-transition phase. Moreover, the coupling between the crystalline and amorphous phases causes a shift in the glass-transition phase to higher temperatures (Righetti, Tombari, & Di Lorenzo, 2008). Consequently, the T_g values for these hydrogels may be at or above the melting point. In this experiment, the detection of T_g was hindered because the temperature range was limited to an upper range of 160 °C based upon the observation of Szczesniak et al. (2008), who reported that cellulose begins to change color from white to yellow-brown above 180 °C.

3.7. Morphological analysis

As shown by the SEM results in Fig. 5, the morphology of the hydrogels depends on the hydrogel composition and irradiation dose, with pore size decreasing with increasing AA content and irradiation dose. This observation supports the previous observation that higher doses of electron-beam irradiation lead to the formation of a greater number of inter-polymeric networks between PAA and BC, resulting in denser networks and smaller pore size (Chauhan & Chauhan, 2008; Da Silva & Ganzarolli de Oliveira, 2007). These morphological observations suggest that the highly porous sponge-like structure of BC/AA hydrogels facilitates the diffusion of water in all directions, making these hydrogels suitable for drug-delivery (Amin, Halib, & Ahmad, 2010). The pore size of the 208050 (20–110 μm), 208035 (60–190 μm) and 307035 (2–50 μm) hydrogels suggested that they are more suitable than the other hydrogels for BSA loading and release studies.

3.8. Swelling studies

The swelling ratios of BC/AA hydrogels are presented in Fig. 6. As can be observed in Fig. 6(a), the hydrogels exhibited a low swelling ratio within acidic medium (pH 2–5) that increased with increasing pH (pH 5–8) until reaching a peak in medium of neutral pH (pH 7). At pH 2, the swelling rate slightly increased between 2 and 8 h of exposure before reaching a swelling equilibrium after 24 h. However, at pH 7, the state of equilibrium could not be determined, as the hydrogel continued to swell beyond 48 h. At pH 10, the swelling rate was slightly higher for the first 8 h compared to that at pH 7, but subsequently decelerated until reaching equilibrium after 24 h. The sensitivity of the response of the hydrogels to changes in pH (from pH 2 to pH 7) was likely due to the hydrophilicity of the carboxylic group in the hydrogel structure. When the pH is increased, the carboxylic group of AA is deprotonated to a negatively charged carboxylate ion (Da Silva & Ganzarolli de Oliveira, 2007; Marchessault & Sundararajan, 1983), with the resulting electrostatic repulsion causing the hydrogel to swell (Akala, Kopeckova, & Kopecek, 1998). However, in an alkaline environment, the hydrogels interact with basic species, restricting the interaction of the water molecules with the acid molecules. The non-ionized condition of the carboxylic groups and the restricted interaction between the water and acid molecules result in a reduction of the swelling ratio,

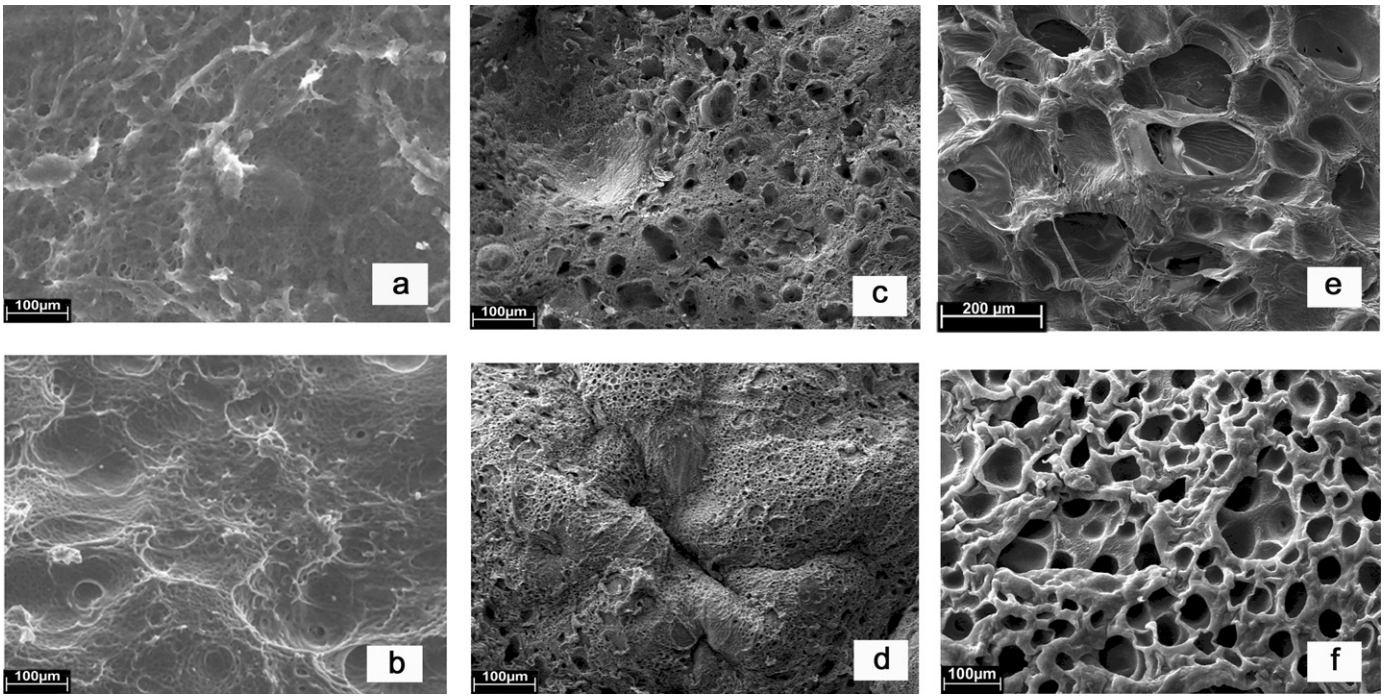

Fig. 5. SEM images of hydrogels: (a) 406035, (b) 406050, (c) 307035, (d) 307050, (e) 208035, and (f) 208050.

particularly at pH values <5 and >10 (Amin et al., 2010; Chauhan & Chauhan, 2008).

The swelling kinetics for the hydrogels at various temperatures is shown in Fig. 6(b). As can be observed, the hydrogels with greater AA content and synthesized at an irradiation dose of 50 kGy swelled to a lesser extent due to their denser structure, which likely restrict mobility within the network (Panda, Manohar, Sabharwal, Bhardwaj, & Majali, 2000). Although all the hydrogels reached their equilibrium state after 24 h, the hydrogels synthesized at 35 kGy exhibited the least swelling at 37 °C, while those synthesized at 50 kGy experienced a reduced swelling percentage at 25 °C. These demonstrated characteristics of thermo- and pH-responsive swelling suggest that these hydrogels are promising candidates for controlled drug-delivery systems, as it suggests that

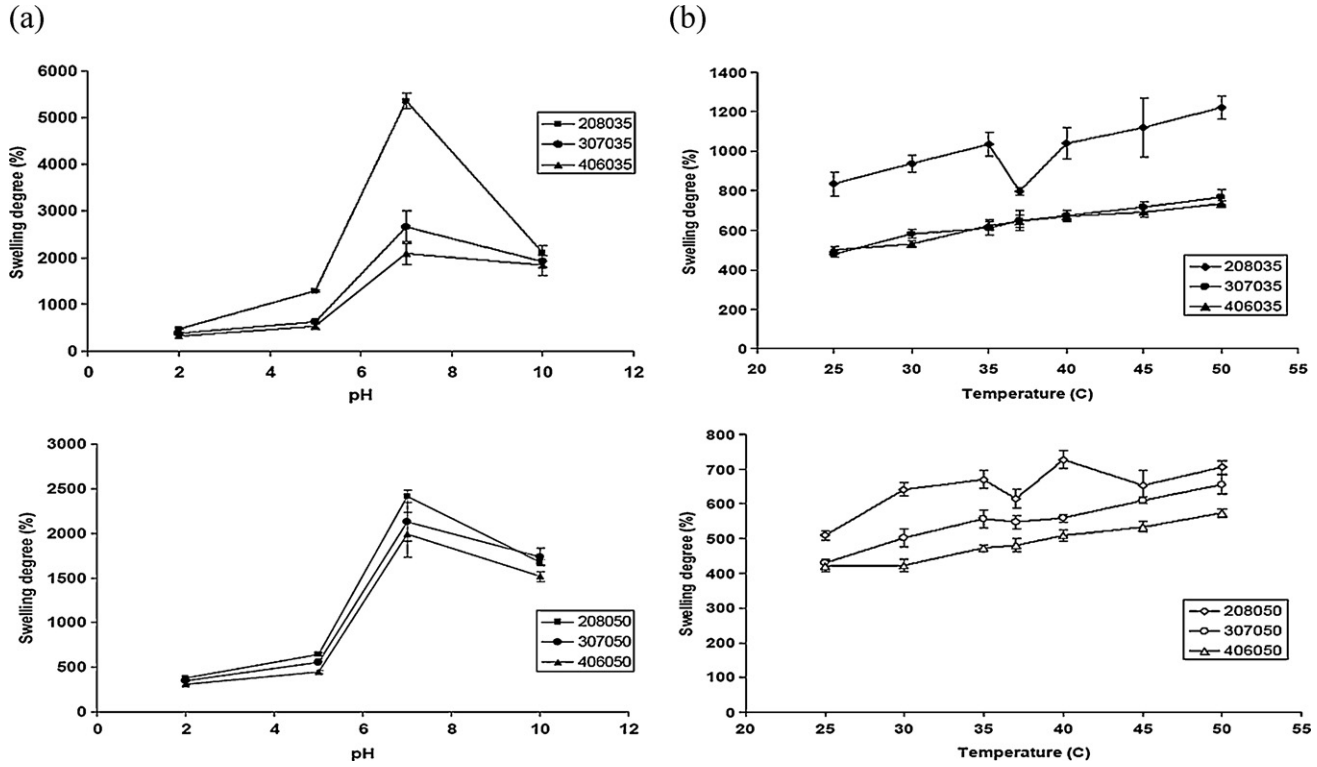

Fig. 6. Swelling behavior of hydrogels: (a) pH response and (b) temperature response.

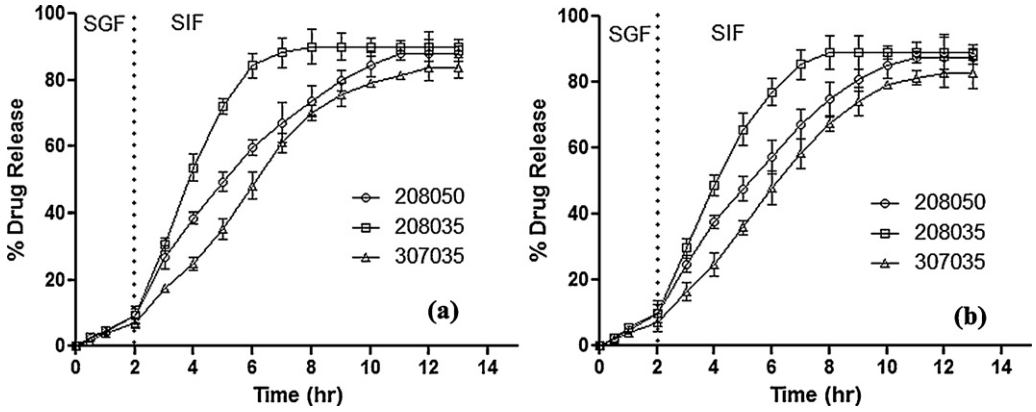

Fig. 7. In vitro drug release profiles of hydrogels: (a) hydrogels loaded with 1% (w/v) BSA and (b) hydrogels loaded with 0.5% (w/v) BSA.

they can be developed in a manner that triggers drug release with any change in pH and body temperature.

3.9. In vitro drug-release studies

The in vitro drug-release profiles of the hydrogels are presented in Fig. 7. The EE of BSA in hydrogels was found to be 36.3%, 48.3% and 55.6% for 307035, 208050 and 208035 hydrogels, respectively. This suggests that the EE was mainly dependent on the pore size of the hydrogels as it was the highest for 208050 and the lowest for 307050 hydrogels. Drug release from a hydrogel mainly depends on the swelling behavior of the hydrogel, the interaction of the drug with the polymers, and the solubility of the drug in the release media (Brazel & Peppas, 1999). The cumulative percentage release of BSA from the hydrogels was lower in the SGF than the SIF, which was mainly due to lower swelling of hydrogel in acidic environment as discussed earlier in Section 3.8. Among all hydrogels, the 307035 showed the lowest release in SGF, which was expected due to its greater AA contents resulting in more pH sensitivity. At initial immersion, the hydrogels released a burst of BSA, which was likely due to the presence of some BSA on the surface of the hydrogels. Since the concentration gradient is the driving force in drug release, the relatively high concentration gradient between the surrounding medium and the surface of the hydrogel at this initial stage was likely to lead the release of BSA (Chiba, Hanes, & Langer, 1998; Gupta, Vermani, & Garg, 2002). The time to reach maximum cumulative percentage release was found to be 8 h for 208035 (≈90%), 11 h for 208050 (≈88%) and 13 h for 307035 (≈83%) hydrogels which was most likely due to the differences in the pore size of the hydrogels. Hydrogels with larger pore size are expected to achieve maximum release sooner than others.

As the drug release from swellable matrices is primarily controlled by diffusion process, hence, Peppas' semi-empirical power law as in Eq. (5) was applied in order to understand the release kinetics of BSA from the hydrogels (Korsmeyer, Gurny, Doelker, Buri, & Peppas, 1983).

$$\frac{M_t}{M_\infty} = kt^n \tag{5}$$

where M_t/M_∞ is the fractional release of drug in time t, k is constant characteristic of drug delivery system and n is the diffusion exponent indicating release kinetic mechanism. The n and k values were calculated from the slope and intercept of the plot of $\ln(M_t/M_\infty \leq 0.6)$ against $\ln t$, respectively and represented in Table 2 along with the regression coefficients. For cylindrical hydrogel disks, when n value equals to 0.45, it corresponds to the Fickian diffusion while when n value is between 0.45 and 0.89, it then represents the non-Fickian diffusion (Ritger & Peppas, 1987). The values of n for BC/AA hydrogels ranged between 0.47 and 0.77 indicating that the absorption of the surrounding medium and the release of BSA via a swelling-controlled diffusion mechanism occurred simultaneously.

Table 2
Diffusion exponent n, constant k and regression coefficient r^2 for BC/AA hydrogels.

Sample	n	k	r^2
208050	0.4646	0.1351	0.9404
208035	0.5663	0.0993	0.9667
307050	0.7669	−0.3022	0.9056

These findings suggest that BC/AA hydrogels exhibit tremendous potential as controlled drug-delivery systems, especially in drugs that degrade in gastric environments, such as protein-based drugs. Due to their lesser extent of swelling at a much lower pH, these hydrogels could protect the drug in the acidic stomach environment (pH 1.2) before releasing it in the small intestine (pH 6.8) for absorption into the systemic circulation.

4. Conclusions

This study explored the potential of a novel hydrogel fabricated from BC, a natural polymer, for application in drug-delivery systems by fabricating a series of BC-based hydrogels by electron-beam irradiation. The results of FT-IR analysis revealed that AA had been successfully grafted onto the cellulose fibers and allowed for prediction of the reaction mechanism in the synthesis of the hydrogels. Morphological analysis revealed that all hydrogels had a highly macroporous sponge-like structure and the pore size of hydrogels decreased with increasing AA content and irradiation doses. DSC analysis suggested that the thermal stability of the hydrogels was suitable for their application as drug-delivery systems.

The results of the swelling studies suggest that the hydrogels were thermo- and pH-responsive, with an initially low swelling ratio at pH 2 increasing with increasing pH, mainly due to the ionization of AA at higher pH values, until reaching a peak at pH 7. Such pH-responsive behavior resulted in a lower in vitro drug-release rate in SGF compared to SIF. The hydrogels showed a reduced swelling at body temperature suggesting that they can be applied for temperature-controlled delivery. These preliminary findings suggest that BC/AA hydrogels could be exploited as components in a controlled delivery system for protein-based drugs. As such, they warrant further investigation into the biodegradability and stability of these hydrogels under simulated conditions.

Acknowledgements

The authors would like to thank Universiti Kebangsaan Malaysia (UKM), the Ministry of Agriculture (MoA), Malaysia, and the Malaysian Nuclear Agency for their support. This project was funded by MoA: Science Fund 05-01-02-SF1023.

References

Akala, E. O., Kopeckova, P., & Kopecek, J. (1998). Novel pH sensitive hydrogels with adjustable kinetics of swelling. *Biomaterials*, *19*, 1037–1047.

Amin, M. C. I. M., Halib, N., & Ahmad, I. (2010). Unique stimuli responsive characteristics of electron beam synthesized bacterial cellulose/acrylic acid composite. *Journal of Applied Polymer Science*, *116*, 2920–2929.

Anjali, P., Manohar, S. B., Sabharwalb, S., Bhardwajb, Y. K., & Majalib, A. B. (2000). Synthesis and swelling characteristics of poly (N-isopropylacrylamide) temperature sensitive hydrogels crosslinked by electron beam irradiation. *Radiation Physics and Chemistry*, *58*, 101–110.

Beneke, C. E., Viljoen, A. M., & Hamman, J. H. (2009). Polymeric plant-derived excipients in drug delivery. *Molecules*, *14*, 2602–2620.

Brazel, C. S., & Peppas, N. A. (1999). Mechanism of solute and drug transport in relaxing, swellable, hydrophilic glassy polymers. *Polymer*, *40*, 3383–3398.

Chan, C. K., & Chu, I. M. (2001). Effect of hydrogen bonding on the glass transition behaviour of poly (acrylic acid)/silica hybrid materials prepared by sol–gel process. *Polymer*, *42*, 6089–6093.

Chauhan, G. S., & Chauhan, S. (2008). Synthesis, characterization, and swelling studies of pH- and thermosensitive hydrogels for speciality applications. *Journal of Applied Polymer Science*, *109*, 47–55.

Chiba, M., Hanes, J., & Langer, R. (1998). Degradation of porous poly(anhydride-co-imide) microspheres and implication for controlled macromolecule delivery. *Biomaterials*, *18*, 163–172.

Czaja, W. K., Young, D. J., Kawecki, M., & Brown, R. M. (2008). The future prospects of microbial cellulose in biomedical applications. *Biomacromolecules*, *8*, 1–12.

Da Silva, R., & Ganzarolli de Oliveira, M. (2007). Effect of the cross-linking density on the morphology of poly(NIPAAm-co-Aac) hydrogels. *Polymer*, *48*, 4114–4122.

Domb, A. J., & Kost, J. (1997). *Handbook of biodegradable polymers*. Amsterdam, The Netherlands: Harwood.

Dubinsky, S., Grader, G. S., Shter, G. E., & Silverstein, M. S. (2004). Thermal degradation of poly(acrylic acid) containing copper nitrate. *Polymer Degradation and Stability*, *86*, 171–178.

El-Naggar, A. W. M., Abd Alla, S. G., & Said, H. M. (2006). Temperature and pH responsive behavior of CMC/AAc hydrogels prepared by electron beam irradiation. *Material Chemistry and Physics*, *95*, 158–163.

Gabbott, P. (2008). *Principles and applications of thermal analysis*. Oxford, UK: Blackwell Publishing.

Grzegorczyn, S., & Slezak, A. (2007). Kinetics of concentration boundary layers buildup in the system consisted of microbial cellulose biomembrane and electrolyte solutions. *Journal of Membrane Science*, *304*, 148–155.

Guenther, U., Smirnova, I., & Neubert, R. H. H. (2008). Hydrophilic silica aerogels as dermal drug delivery systems – Dithranol as a model drug. *European Journal of Pharmaceutics and Biopharmaceutics*, *69*, 935–942.

Gupta, P., Vermani, K., & Garg, S. (2002). Hydrogels: From controlled release to pH responsive drug delivery. *Drug Discovery Today*, *7*, 569–579.

Hamidi, M., Azadi, A., & Rafiei, P. (2008). Hydrogel nanoparticles in drug delivery. *Advanced Drug Delivery Reviews*, *60*, 1638–1649.

Haraguchi, K., Takehisa, T., & Fan, S. (2002). Effects of clay content on the properties of nanocomposite hydrogels composed of poly(N-isopropylacrylamide) and clay. *Macromolecules*, *35*, 10162–10171.

Hennink, W. E., De Jong, S. J., Bos, G. W., Veldhuis, T. F. J., & Van Nostrum, C. F. (2004). Biodegradable dextran hydrogels crosslinked by stereocomplex formation for the controlled release of pharmaceutical proteins. *International Journal of Pharmaceutics*, *277*, 99–104.

Hennink, W. E., & van Nostrum, C. F. (2002). Novel crosslinking methods to design hydrogels. *Advanced Drug Delivery Reviews*, *54*, 13–36.

Hong, F., & Qiu, K. (2008). An alternative carbon source from konjac powder for enhancing production of bacterial cellulose in static cultures by a model strain *Acetobacter aceti* subsp. *xylinus* ATCC 23770. *Carbohydrate Polymers*, *72*, 545–549.

Hua, W., Chena, S., Lia, X., Shia, S., Shena, W., Zhanga, X., et al. (2009). In situ synthesis of silver chloride nanoparticles into bacterial cellulose membranes. *Materials Science and Engineering*, *27*, 1216–1219.

Huang, M. R., & Li, X. G. (1998). Thermal degradation of cellulose and cellulose esters. *Journal of Applied Polymer Science*, *68*, 293–304.

Karaaslana, M. A., Tshabalalab, M. A., Yelleb, D. J., & Buschle-Diller, G. (2011). Nanoreinforced biocompatible hydrogels from wood hemicelluloses and cellulose whiskers. *Carbohydrate Polymers*, *86*, 192–201.

Korsmeyer, R. W., Gurny, R., Doelker, E. M., Buri, P. L., & Peppas, N. A. (1983). Mechanism of solute release from porous hydrophilic polymers. *International Journal of Pharmaceutics*, *15*, 25–35.

Lau, C., & Mi, Y. (2002). A study of blending and complexation of poly (acrylic acid)/poly (vinyl pyrrolidone). *Polymer*, *43*, 823–829.

Malafaya, P. B., Silva, G. A., & Reis, R. L. (2007). Natural-origin polymers as carriers and scaffolds for biomolecules and cell delivery in tissue engineering applications. *Advanced Drug Delivery Reviews*, *59*, 207–233.

Marchessault, R. H., & Sundararajan, P. R. (1983). *The polysaccharides*. New York, NY: Academic Press.

Moreira, S., Silva, N. B., Almeida-Lima, J., Rocha, H. A. O., Medeiros, S. R. B., Alves, C., et al. (2009). BC nanofibres: In vitro study of genotoxicity and cell proliferation. *Toxicology Letters*, *189*, 235–241.

Nada, A. M. A., & Hassan, M. L. (2007). Thermal behavior of cellulose and some cellulose derivatives. *Polymer Degradation and Stability*, *67*, 111–115.

Panda, A., Manohar, S. B., Sabharwal, S., Bhardwaj, Y. K., & Majali, A. B. (2000). Synthesis and swelling characteristics of poly(N-isopropylacrylamide) temperature sensitive hydrogels crosslinked by electron beam irradiation. *Radiation Physics and Chemistry*, *58*, 101–110.

Patel, U. D., & Suresh, S. (2008). Complete dechlorination of pentachlorophenol using palladized bacterial cellulose in a rotating catalyst contact reactor. *Journal of Colloid and Interface Science*, *319*, 462–469.

Pavia, D. L., Lampman, G. M., & Kriz, G. S. (2001). *Introduction to spectroscopy*. New York, NY: Thomson Learning.

Peppas, N. A., Bures, P., Leobandung, W., & Ichikawa, H. (2000). Hydrogels in pharmaceutical formulations. *European Journal of Pharmaceutics and Biopharmaceutics*, *50*, 27–46.

Righetti, M. C., Tombari, E., & Di Lorenzo, M. L. (2008). Crystalline, mobile amorphous and rigid amorphous fractions in isotactic polystyrene. *European Polymer Journal*, *44*, 2659–2667.

Ritger, P. I., & Peppas, N. A. (1987). A simple equation for description of solute release. II. Fickian and anomalous release from swellable devices. *Journal of Controlled Release*, *5*, 37–42.

Said, H. M., Abd Alla, S. G., & El-Naggar, A. W. M. (2004). Synthesis and characterization of novel gels based on carboxymethyl cellulose/acrylic acid prepared by electron beam irradiation. *Reactive & Functional Polymers*, *61*, 397–404.

Säkkinen, M., Seppälä, U., Heinänen, P., & Marvola, M. (2002). In vitro evaluation of microcrystalline chitosan (MCCh) as gel-forming excipient in matrix granules. *European Journal of Pharmaceutics and Biopharmaceutics*, *54*, 33–40.

Scherzer, T., Beckert, A., Langguth, H., Rummel, S., & Mehnert, R. (1998). Electron beam curing of methacrylated gelatin. I. Dependence of the degree of crosslinking on the irradiation dose. *Journal of Applied Polymer Science*, *63*, 1303–1312.

Strauss, P., Knolle, W., & Naumov, S. (1998). Radiation-induced radical formation and crosslinking in aqueous solutions of N-isopropylacrylamide. *Macromolecular Chemistry and Physics*, *199*, 2229–2235.

Szczesniak, L., Rachocki, A., & Tritt, G. J. (2008). Glasss transition temperature and thermal decomposition of cellulose powder. *Cellulose*, *15*, 445–451.

Takács, E., Dajka, K., & Wojnárovits, L. (2001). Study of high-energy radiation initiated polymerization of butyl acrylate. *Radiation Physics and Chemistry*, *63*, 41–44.

Tatsuya, O., Sachiko, T., Kaoru, O., & Yoshinari, B. (2011). Phosphorylated bacterial cellulose for adsorption of proteins. *Carbohydrate Polymers*, *83*, 953–958.

Ulański, P., Bothe, E., Rosiak, J., & von Sonntag, C. (1994). OH-radical-induced crosslinking and strand breakage of poly(vinyl alcohol) in aqueous solution in the absence and presence of oxygen. A pulse radiolysis and product study. *Macromolecular Chemistry and Physics*, *195*, 1443–1461.

Wang, Y., Luo, Q., Peng, B., & Pei, C. (2008). A novel thermotropic liquid crystalline benzoylated bacterial cellulose. *Carbohydrate Polymers*, *74*, 875–879.